

A toy model to understand the dynamics of the vortical motions in turbulent boundary layers

J.C. Cuevas Bautista*

University of New Hampshire, Department of Mechanical Engineering, Durham 03824, USA.

(Dated: April 5, 2016)

Recent studies indicate that the structure of the turbulent boundary layer at high Reynolds number (Re) is composed of large uniform momentum zones segregated by fissures of concentrated vorticity. Experiments reveal that the dimensionless fissures thickness (scaled by boundary layer thickness) is $\mathcal{O}(1/\sqrt{Re})$ and the dimensionless streamwise velocity jump across a fissure scales with the friction velocity $\mathcal{O}(u_\tau)$. A toy model that captures the essential elements of the turbulent boundary layer structure at high Re is constructed to evaluate the long-time averaged flow statistics of the boundary layer. First, a “master” instantaneous streamwise velocity profile in the wall-normal direction is constructed by placing a discrete number of fissures across the boundary layer thickness. The number of fissures and their wall-normal locations follow scalings informed by the Mean Momentum Balance (MMB) theory. Next, the wall-normal positions of the fissures are allowed to randomly move in the wall-normal direction creating a statistically independent second instantaneous velocity profile. This process is then repeated to create an ensemble of instantaneous velocity profiles from which average statistics of the turbulent boundary layer can be computed and assessed. The statistics of the toy model are compared to statistics acquired in turbulent boundary layers at high Re .

I. NUMERICAL METHODS

A step master stream-wise velocity profile is represented by a set of discrete steps uniformly spaced according with Eqs. 1 and 2,

$$U_{i+1}^+ = U_i^+ + \phi_c^2 \ln(\phi_c), \quad (1)$$

$$y_{i+1}^+ = \phi_c y_i^+. \quad (2)$$

These relationships are derived from the MMB theory [1], where Eq. 1 determine the increments in the stream-wise normalized velocity U^+ , the width of the steps in the x coordinate and Eq. 2 determine the increments in the normalized wall normal position y^+ , the height of the steps in the y coordinate (See Fig. 1). The constant factor ϕ_c is given by $\phi_c = (1 + \sqrt{5})/2$ and since the thickness of the vortical fissures scales like $\mathcal{O}(1/\sqrt{Re})$, it is considered negligible at high Re . The initial wall normal position was set to $y_0^+ = \phi_c \sqrt{\delta^+}$ in order to match with the onset of the logarithmic region according with the MMB theory and $U_0^+ = 0.5U_\infty^+$ to be the half of the normalized free-stream velocity U_∞^+ .

The last position y_N^+ of the vortical fissure and its associated velocity U_N^+ is bounded by the turbulent boundary layer thickness δ or its respective Reynolds number $\delta^+ = \frac{\delta}{\nu/u_\tau}$, where $u_\tau = \sqrt{\tau_\omega/\rho}$ is the friction velocity (τ_ω is the mean wall shear stress and ρ is the mass density respectively) and ν is the kinematic viscosity. Fig. 1 depicts the step master turbulent velocity profile with a grid of 5481 linearly spaced positions in the wall normal direction each one associated to a streamwise velocity.

The dot circles are the positions and velocities of the vortical fissures computed using Eqs. 2 and 1 respectively. The zones of uniform momentum are created allocating the same velocity of the vortical fissure to the grid points between the previous vortical fissure and the current vortical fissure. This velocity remains characteristic for each vortical fissure, thus the number of vortical fissures establishes the number of uniform momentum zones. Then instantaneous multiple velocity profiles are created by simulate a random motion in the wall normal direction of the vortical structures. This is accomplished by add a Gaussian perturbation of the actual height of the uniform momentum zone to the current position of the vortical fissure (black dots in Fig. 1) in the step turbulent master profile. Once the new wall normal positions

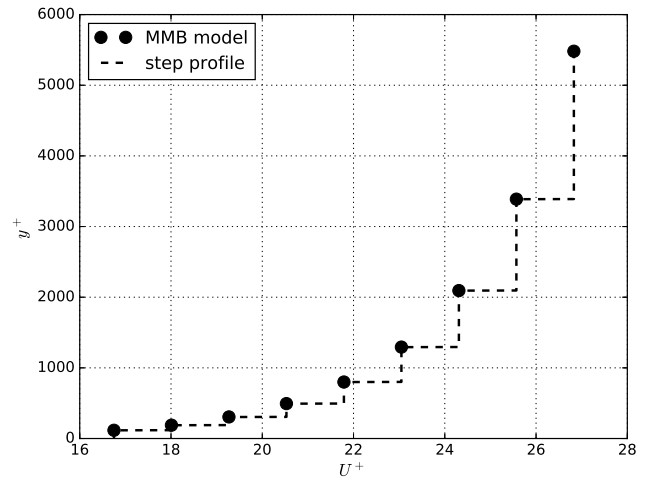


FIG. 1. Step turbulence master profile for $\delta^+ = 5200$ and $U_\infty^+ = 26.5$.

* jcc1@wildcats.unh.edu

have been computed, the grid velocity is filled with the attached velocity of each vortical fissure corresponding to their new wall normal positions. This physically means that the vortical fissures can cross each other through the turbulent boundary layer step profile generating zones of negative vorticity. Fig. 2 shows five instantaneous turbulent velocity step profiles, it can be seen how the vortical fissures changes their position trough the turbulent boundary layer for the different profiles. The time units in Fig. 2 are arbitrary, i.e. they just illustrate different instants of time. The multiple instantaneous step velocity profiles are considered independent events since they are the result of the Gaussian perturbation in the wall normal positions of the master profile. Thus to achieve statistical convergence the mean turbulent stream-wise velocity profile is constructed by average over 5000 independent realizations.

II. MEAN TURBULENCE STATISTICS ANALYSIS

For the purpose of validate the toy model, the high order moments such as the mean, variance, skewness and kurtosis of the mean turbulent streamwise velocity profile were computed. As described in Sec. I, not only a Gaussian perturbation was used to randomize the positions of the vortical fissure but also an uniform distribution. These variations attempts to explore if there is a dependence between the perturbation distribution and the statistics of the toy model. Thus a strong agreement between the numerical results either for any perturbation and the experimental data could give us some insight about the statistical nature of this process in a real turbulent flow.

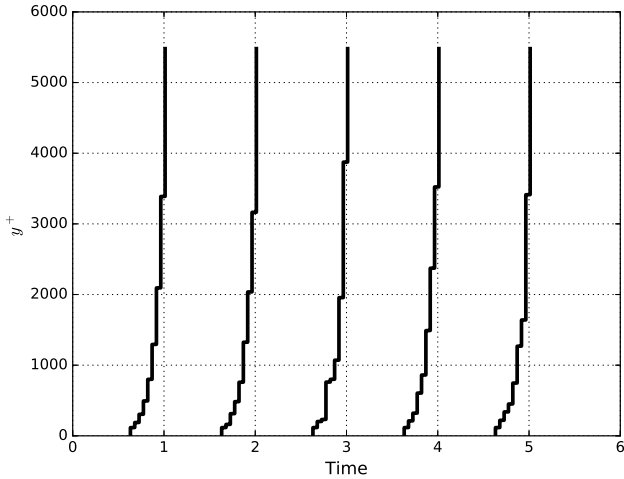


FIG. 2. Multiple instantaneous velocity profiles with a gaussian perturbation of mean $\mu = 0$ and standard deviation $\sigma = 0.4$.

A. Gaussian perturbation

Multiple scenarios with different standard deviations were investigated for the Gaussian perturbation, however just two are presented here. They represent poor $\sigma = 0.4$ and good $\sigma = 1$ agreement with the experimental results [2, 3], both with $\mu = 0$. First scenario considers that the random variation in the position of the vortical fissures ranges between -120% and 120% of their current positions, where 3σ events are less likely to occur. Fig. 3 is the turbulent mean velocity profile for $\sigma = 0.4$. It can be appreciated regions of relative uniform velocity along with small velocity jumps located close to the unperturbed wall normal positions of the vortical fissures (see Fig. 1). These oscillations are similar to the peak-locking phenomena in experimental data, and they are the result of the velocity average of vortical fissures with identical velocities in the same wall normal positions. Also note that an uniform momentum zone arise from $y^+ = 0$ to $y^+ = 116$, these are the velocity boundary conditions imposed in the first position of the vortical fissure which are held fixed. Despite of these discrepancies, the mean velocity profile shows an acceptable agreement with the shape of the experimental data.

Fig. 4 shows the variance of the streamwise fluctuations for 5000 independent realizations as a function of the wall normal position. Here the peak-locking phenomena is more evident and it could be associated to the use of pseudo-random number generators (PRNG). Since the Gaussian random numbers are not totally independent but they are computed through a deterministic algorithm, wall normal positions can be populated with the same vortical fissures several times [4]. It is also remarkable that for this scenario crossing vortical fissures are rarely observed since the random perturbation does not

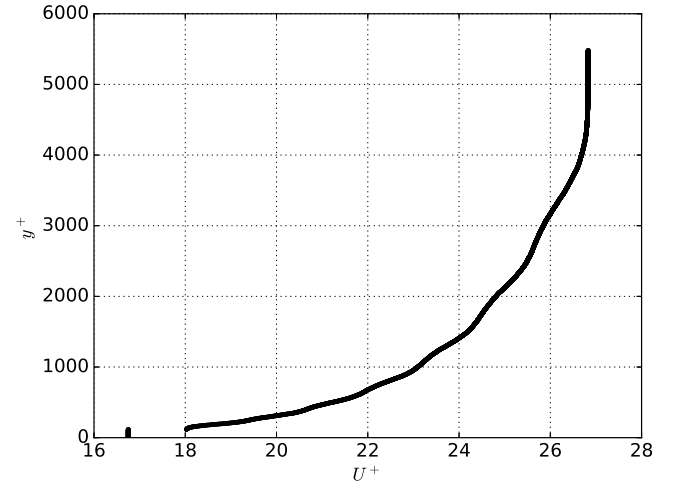


FIG. 3. Mean stream-wise velocity profile for 5000 independent realizations with a Gaussian perturbation of $\mu = 0$ and $\sigma = 0.4$.

exceed 130% units of their current wall normal positions.

As is usual Fig. 5 shows the skewness for the stream-wise fluctuations as a function of the wall normal position on a semi-logarithmic axes plot. It shows the right tendency for wall normal positions close to the wall and in the boundary edge. However in the logarithmic region the skewness oscillates around the Gaussian value, these rapid variations are caused by clustering effect. Unlike the skewness (Fig 5), the stream-wise velocity kurtosis oscillations are higher if they are compared with the Gaussian distribution where the kurtosis is equal to 3. This behaviour does not reproduce accurately the turbulence statistics and thus we explore higher values of σ in the Gaussian perturbation.

In the second scenario $\sigma = 1$, hence the random motion of the vortical fissures range between -300% and 300% of their respective height of the step (see I). Fig 7. shows a smoother profile compared with the first scenario where clustering effect was evidenced. These mean velocity profile exhibit the right trend for $\delta^+ = 5200$, the constant velocity close to the wall ($y^+ = 0 - 118$) is a consequence of the boundary conditions where the first step velocity is held fixed. In addition to the mean, the second, third and fourth order moments are also computed for this scenario. The stream-wise velocity variance as a function of y^+ is shown in Fig 8.

It can be seen that the variance start to exhibit the right trend, namely zero near to the wall with its maximum value in the onset of the logarithmic region and then decrease almost logarithmically toward the boundary layer edge. Also note that there is not evidence of clustering effect, since a wider range in the vertical perturbations allow the vortical fissures to cross through the boundary layer creating a more homogeneous distribution of the stream-wise velocity. Fig 9 shows the skewness for $\sigma = 1$,

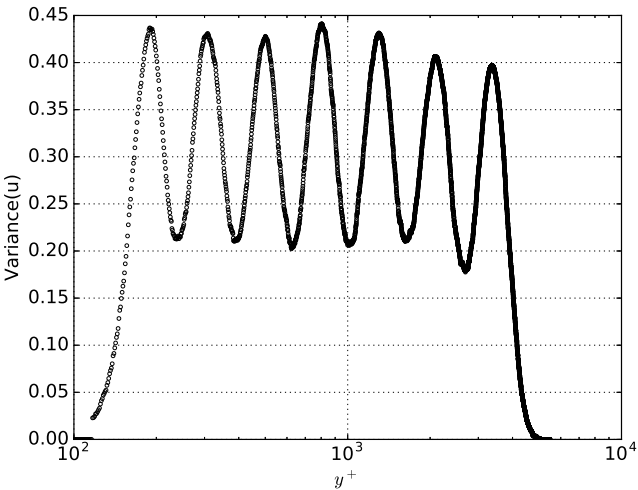


FIG. 4. Stream-wise velocity variance for 5000 independent realizations with a Gaussian perturbation of $\mu = 0$ and $\sigma = 0.4$.

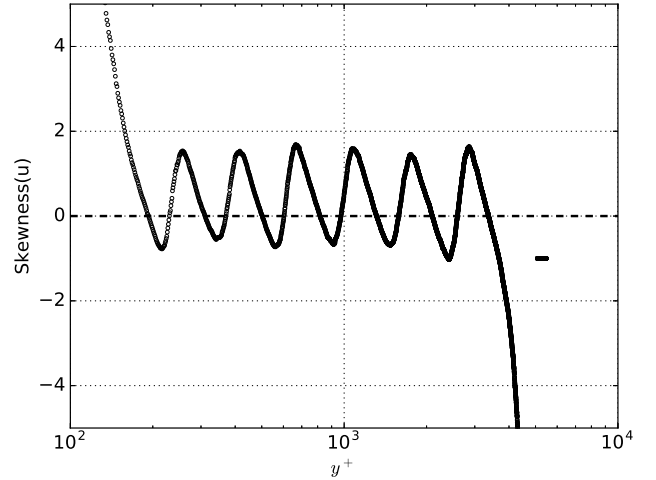


FIG. 5. Stream-wise velocity skewness for 5000 independent realizations with a Gaussian perturbation of $\mu = 0$ and $\sigma = 0.4$ (open circles). The skewness for a Gaussian distribution is plotted in dotted lines as a reference.

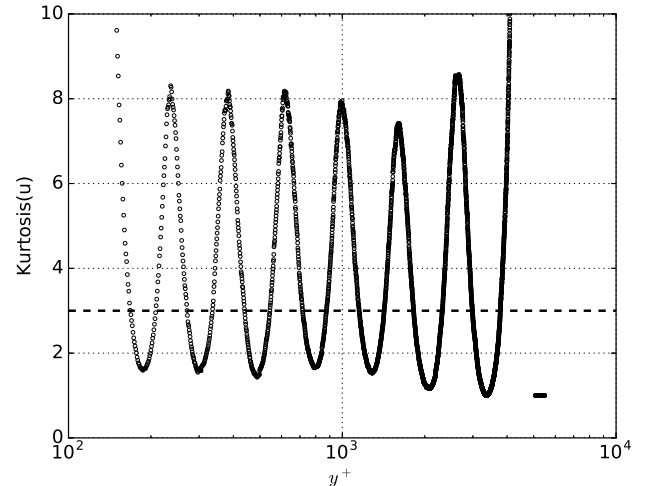


FIG. 6. Stream-wise velocity kurtosis for 5000 independent realizations with a Gaussian perturbation of $\mu = 0$ and $\sigma = 0.4$ (open circles). The kurtosis for a Gaussian distribution is plotted in dotted lines as a reference.

it can be seen how the skewness has its maximum positive value close to the wall and then when it is approaching to the log region it exhibits a Gaussian behaviour to raise up to its maximum negative value at the end of the logarithmic region. Unlike the experimental results for a turbulent skewness, the boundaries don't have the right trend. This is caused mainly because the first and last step in our model are not being perturbed. Further investigation is necessary to establish the proper boundary conditions in order to reproduce the real tendency in the boundaries for the skewness. A similar pattern can be seen for the streamwise kurtosis (Fig 10), where the tendency in the boundaries does not reproduce accurately

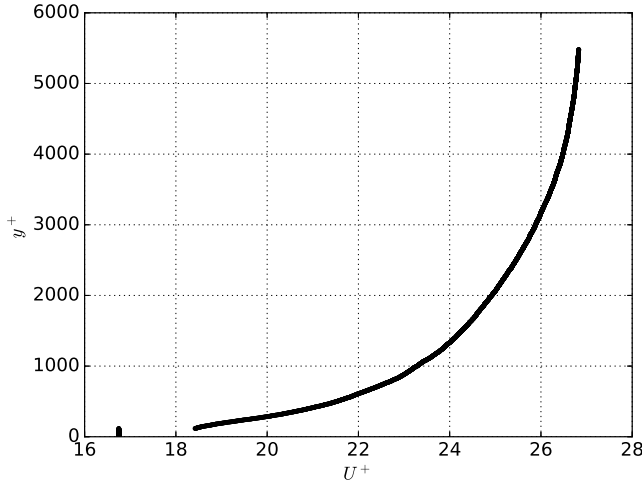


FIG. 7. Mean turbulent stream-wise velocity profile for 5000 independent realizations with a Gaussian perturbation of $\mu = 0$ and $\sigma = 1$.

the experimental results. However in the logarithmic region the kurtosis exhibits a subgaussian trend just as the real data does. For $y^+ = \delta^+$ is expected that the kurtosis reach its maximum value and then decays in the free-stream region for the flow. This suggest that a different distribution can be used to perturb the position of the vortical fissures which edges decays smoother than the gaussian distribution. Thus a uniform distribution is explored in the next section, which attempts to avoid this undesirable tendency in the boundaries of the turbulent boundary layer.

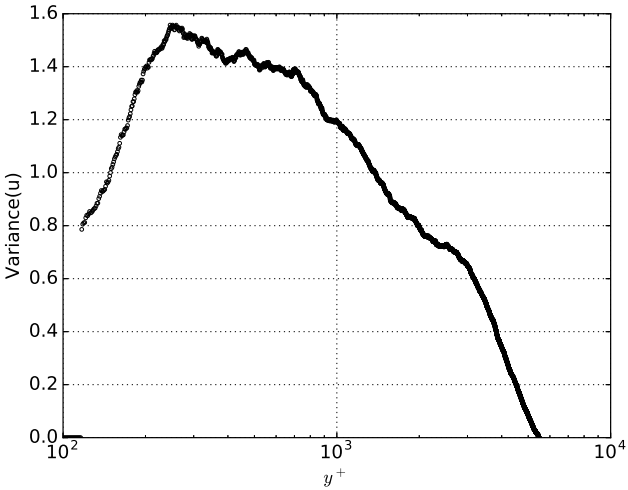


FIG. 8. Stream-wise velocity variance for 5000 independent realizations with a Gaussian perturbation of $\mu = 0$ and $\sigma = 1$.

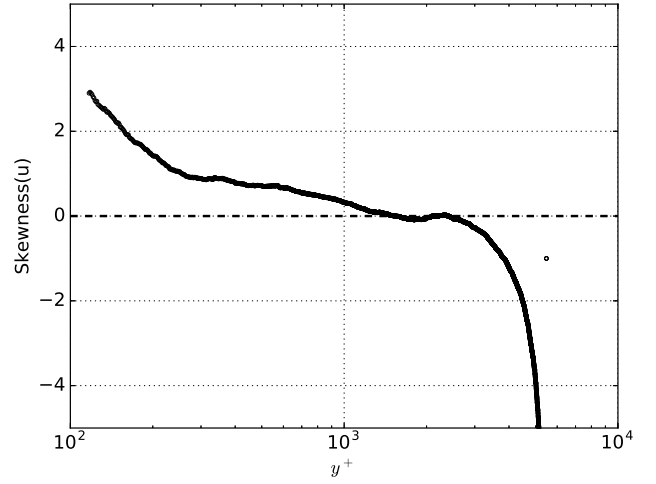


FIG. 9. Skewness of streamwise velocity fluctuations for 5000 independent realizations with a Gaussian perturbation of $\mu = 0$ and $\sigma = 1$ (open circles). The skewness for a Gaussian distribution is plotted in dotted lines as a reference.

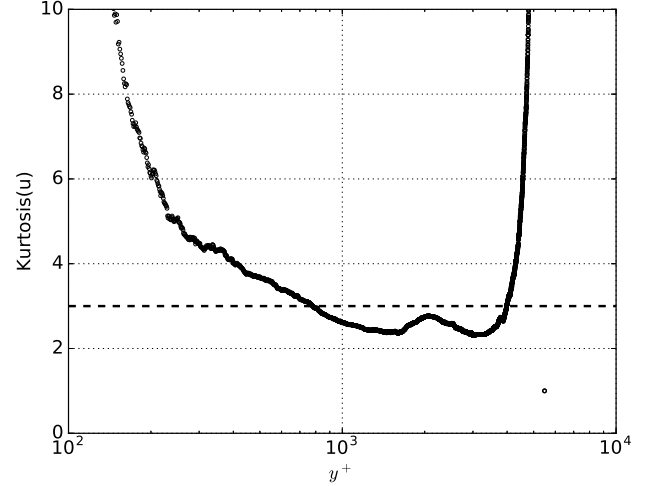


FIG. 10. Kurtosis of streamwise velocity fluctuations for 5000 independent realizations with a Gaussian perturbation of $\mu = 0$ and $\sigma = 1$ (open circles). The kurtosis for a Gaussian distribution is plotted in dotted lines as a reference.

B. Uniform distribution

In order to allow vortical fissure crossing a uniform distribution between -130% and 130% of the height of the step was selected. Fig 11 shows the streamwise velocity profile for this perturbation. Unlike Fig 3, the jumps in the velocity profile seems to have a more straight slope. This is a direct consequence to perturb the vortical fissure positions with an uniform perturbation. This effect can be appreciated more clearly in the stream-wise velocity variance (Fig. 12), where the oscillations are around the vortical fissures of the master profile and have a lower amplitude (~ 0.2 units) compared with the Gaussian dis-

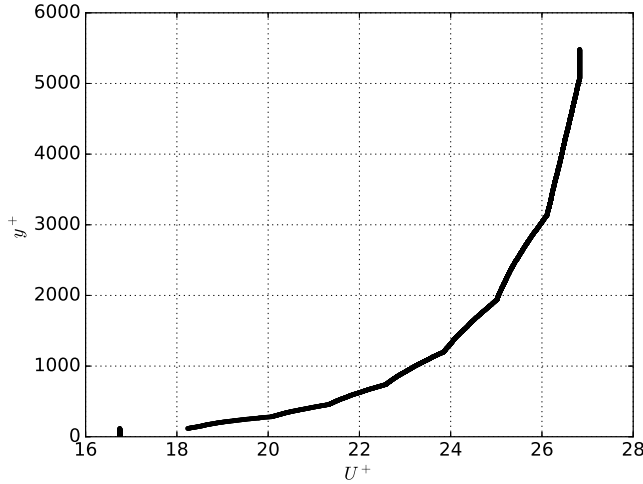


FIG. 11. Mean turbulent stream-wise velocity profile for 5000 independent realizations with an uniform perturbation of $\pm 130\%$.

tribution for a small perturbation (Fig. 4). Despite of the oscillations, the main characteristics of the turbulence variance are conserved. For instance it has a peak in the proximity of the wall and then a pronounced decreasing slope in the inertial region up to reach zero in the boundary layer edge. These oscillations still persists

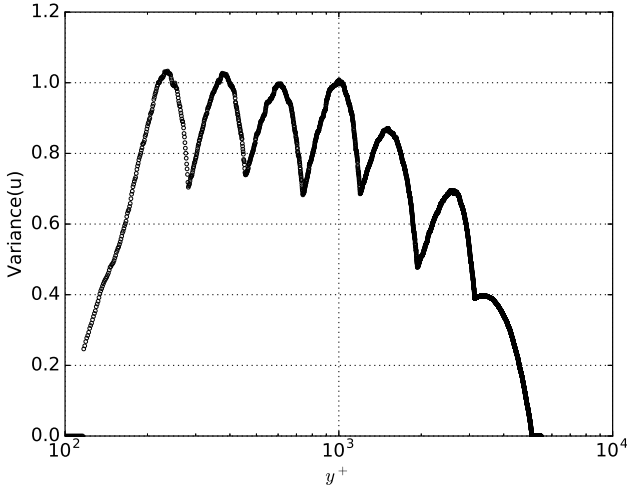


FIG. 12. Variance of streamwise velocity fluctuations for 5000 independent realizations with an uniform perturbation of $\pm 130\%$.

in the higher order moments, however their amplitude is small. Fig. 13 shows the skewness of the streamwise velocity for an uniform distribution. Furthermore the trend of the skewness is similar to the real skewness, namely it

follows a pseudo-Gaussian tendency in the inertial region , then it increases up to reach its maximum negative value next to the boundary layer $y^+ = \delta^+$ and finally decay to zero in the free-stream region. Our model register few

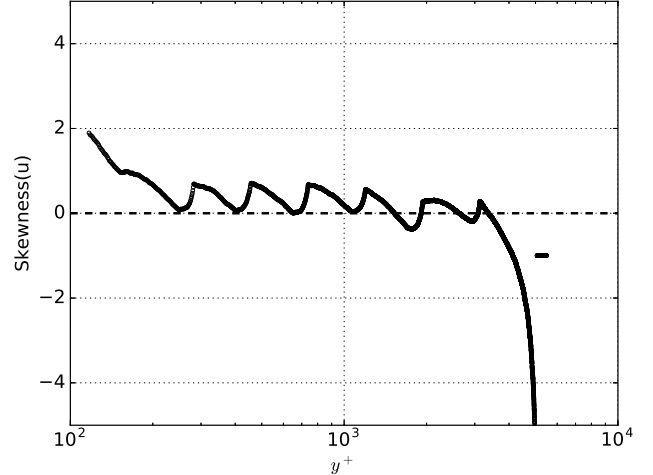


FIG. 13. Skewness of streamwise velocity fluctuations for 5000 independent realizations with an uniform perturbation of $\pm 130\%$ (open circles). The skewness for a Gaussian distribution is plotted in dotted lines as a reference.

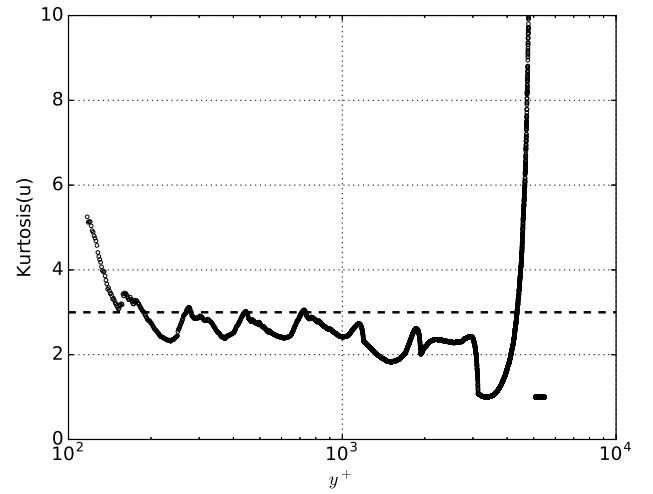


FIG. 14. Kurtosis of streamwise velocity fluctuations for 5000 independent realizations with an uniform perturbation of $\pm 130\%$ (open circles). The kurtosis for a Gaussian distribution is plotted in dotted lines as a reference.

grid points to decay into the free-stream region. Fourth order moment is illustrated in Fig. 14, the tendency is in completely agreement with the real data if the small oscillations are omitted. Further exploration is needed to improve the right tendency in the boundary layer limits, since the first and last vertical position has not been perturbed.

-
- [1] J. Klewicki, P. Fife, T. Wei, and P. McMurtry, Philosophical Transactions of the Royal Society of London A: Mathematical, Physical and Engineering Sciences **365**, 823 (2007).
 - [2] P. Vincenti, J. Klewicki, C. Morrill-Winter, C. M. White, and M. Wosnik, Experiments in Fluids **54**, 1 (2013).
 - [3] J. F. Morrison, B. J. McKeon, W. Jiang, and A. J. Smits, Journal of Fluid Mechanics **508**, 99 (2004).
 - [4] T. Sauer, *Numerical Analysis*, 2nd ed. (Pearson, Boston, MA, 2011).